THE JOURNAL OF PHYSICAL CHEMISTRY C

Article

pubs.acs.org/JPCC

Probing Porous Structure of Single Manganese Oxide Mesorods with Ionic Current

Trevor Gamble,[†] Eleanor Gillette,[‡] Sang Bok Lee,*[,‡] and Zuzanna S. Siwy*[,†]

[†]Department of Physics and Astronomy, University of California, Irvine, California 92697, United States

[‡]Department of Chemistry and Biochemistry, University of Maryland, College Park, Maryland 20742, United States

Supporting Information

ABSTRACT: Characterization of materials in confined spaces, rather than attempting to extrapolate from bulk material behavior, requires the development of new measurement techniques. In particular, measurements of individual meso- or nanoscale objects can provide information about their structure which is unavailable by other means. In this report, we perform measurements of ion currents through a few hundred nanometer long MnO_2 rods deposited in single polymer pores. The recorded current confirms an existence of a meshlike character of the MnO_2 structure and probes the effective size of the mesh voids and the polarity of surface charges. The recorded ion current through deposited MnO_2 structure also suggests that the signal is mostly due to metal cations and not to protons. This is the first time that ionic current measurements have been used to characterize mesoporous structure of this important electrode material.

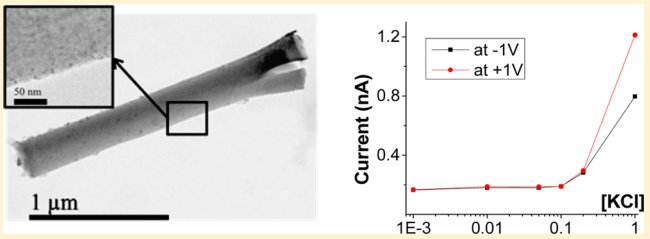

1. INTRODUCTION

Metal oxides are important materials for electrochemical energy storage devices,[1] including lithium ion batteries[2] and supercapacitors,[3] which are receiving increased attention as valuable technologies not only in portable electronics but also in transportation, grid level storage, and other applications. Research on the improvement of oxide materials for energy storage has been primarily focused on the introduction of nanoscale features[3−5] with the goal of increasing specific surface area and decreasing the length of ion diffusion pathways. Specific surface area of electrodes can be measured by gas adsorption or can be estimated geometrically, but these approaches do not give information on whether the determined area is fully accessible to relevant solvated ions. Additionally, direct measurement of ion diffusion through metal oxide nanomaterials can be quite challenging. Given the diverse morphologies, crystal structures, and oxidation states in which many metal oxides can be produced, there is a need for a specific method for probing ion transport in these materials.

Manganese oxide is a popular energy storage material which has been used in lithium ion batteries[6−8] as well as in supercapacitors.[9,10] It features good capacity, earth abundance, low toxicity, and low cost, and there are numerous methods for synthesizing different types of manganese oxide for use in energy storage devices. While the physical properties, like electrical conductivity and crystal structure, are relatively easy to determine, very little has been done to understand how the porous character of MnO_2 influences transport of lithium and other ions inside and through the material. Additionally, there is ongoing uncertainty as to the mechanism of energy storage in various MnO_2 materials, particularly in respect to the contribution of Li^+ or other metal cations as opposed to protons.

In this manuscript, we present a novel method for determining ion transport through a metal oxide using electrodeposited amorphous manganese oxide as a demonstration material. This method takes advantage of the properties of the electrochemical double layer and has been previously applied to polymer nanopores and biological channels.[11−13] Here, for the first time, this method is applied to a nanoporous structure of manganese oxide deposited as a mesorod inside a single, several hundred nanometer in diameter pore in a polymer film of polyethylene terephthalate (PET). Using this method, we were able to confirm the existence of nanovoids in the oxide and were able to determine the effective size of the voids, the type of surface charges, and which ion dominates the measured current signal. Thus, the recorded current through the porous structure of MnO_2 was a direct probe of geometrical and electrochemical properties of the MnO_2 mesorods. Observed saturation of ion currents at low salt concentrations suggests that the voids have effective opening diameter of less than 5 nm and that they also carry negative surface charge. The nanometer character of the charged voids makes them cation selective, which was confirmed by the measurements of the so-called reversal potential: a potential difference established when a porous structure is in contact with a salt concentration gradient.[14]

Received: August 13, 2013
Revised: November 4, 2013
Published: November 4, 2013

   dx.doi.org/10.1021/jp408107z | J. Phys. Chem. C 2013, 117, 24836−24842

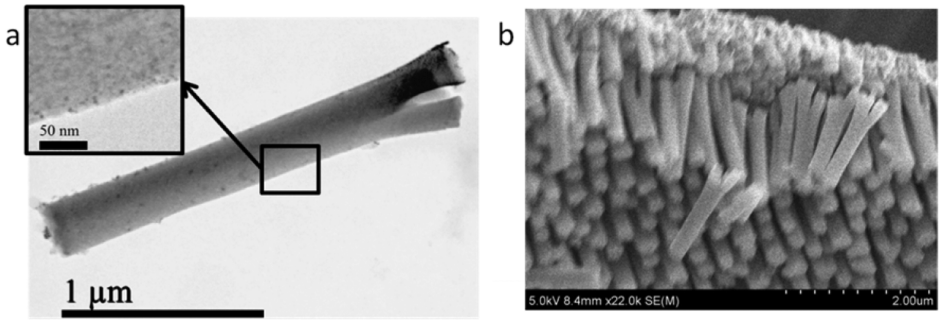

Figure 1. (a) Transmission electron microscopy (TEM) and (b) SEM images of representative MnO_2 rods electrodeposited in anodized aluminum oxide (AAO) pores. The bifurcation observed in the rods is a result of pore branching in the AAO template, created on one side of the membranes during their fabrication process (anodization), and is not expected to be present in the mesorods grown in single pores in PET membranes.

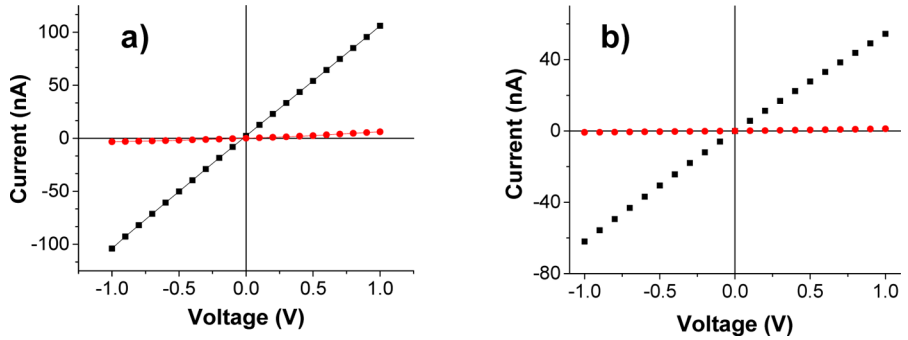

Figure 2. Current–voltage curves through two cylindrical nanopores before (black squares) and after (red circles) deposition of 200 nm long manganese oxide rods. The single cylindrical pores had the original opening diameter of (a) 374 nm and (b) 304 nm. All recordings were performed in 1 M KCl, pH 8. The presented data are averages over three independent voltage scans. The error bars are smaller than the symbols.

2. EXPERIMENTAL METHODS

Preparation of Pores. Single pores in polyethylene terephthalate (PET) films were prepared by the track–etching technique.[15] In the first step, 12 μm thick foils were irradiated with single Au ions of total kinetic energy of ~2 GeV (linear accelerator, GSI, Darmstadt, Germany).[16] In the second step, the irradiated films were etched in 0.5 M NaOH at 70 °C; 30 min of etching in these conditions causes preparation of pores with an average diameter of 100 nm.[17] Pore diameter increases with the etching time in a linear fashion.[15] A more precise estimation of the pore diameter is performed by measuring current–voltage curves in 1 M KCl and by relating the pore resistance with its geometry. Assuming a cylindrical shape of a pore, the pore conductance, G, is given as $G = (k\pi d^2)/(4L)$ where d is the pore-opening diameter, L is the pore length, and k is the conductivity of the solution in the pore. Pores used in the reported experiments had opening diameters between 50 and 400 nm, and thus, the conductivity of the medium in the pore could be assumed equal to the conductivity of a bulk solution, 10 S/m for 1 M KCl. All current–voltage curves were recorded in a conductivity cell whose two chambers were separated by a single pore membrane. Two nonpolarizable Ag/AgCl electrodes were used in the measurements. Measurements in symmetric electrolyte conditions were performed with Ag wires with deposited AgCl. Recordings in asymmetric salt concentrations were performed with homemade Ag/AgCl electrodes immersed in agar saturated with 3 M KCl. The agar electrodes were prepared as described in the literature.[18,19] Briefly, 0.5 mL of a heated solution of 4 g agar in 100 mL of 3 M KCl was suctioned into a 1 mL eppendorf pipet tip; the remaining volume of the pipet was filled with 3 M KCl. The electrodes were reported to perform very well for measuring small currents with high precision, and no leakage of the electrolyte from the electrode was observed.[18,19] The high concentration of 3 M KCl in the agar electrodes also reduces the junction potential to values below 2 mV.[20] All electrolyte solutions were prepared in deionized water and were buffered to pH 8 using Tris buffer.

Deposition of Rods. Manganese oxide rods were prepared within PET pores using electrodeposition. First, one side of a PET membrane containing a single pore was sputtered with ~200 nm thick layer of gold using a Denton Desktop III coating system (Denton Vacuum LLC, Moorestown, NJ). The gold layer blocked one entrance of the pore, providing an electroactive surface for the growth of MnO_2 in the pore. A ring of copper tape (3M) was used to connect the gold side of the film to the external circuit and to provide mechanical support for the membrane. The copper ring and the membrane were sealed in acid-free tape (3M), which restricted electrolyte access to the conductive copper surface and which limited the deposition only to the interior of the pore. Electrodeposition was carried out using a bipotentiostat (BioLogic, Claix, France) in a three-electrode cell with a platinum counter electrode and a Ag/AgCl reference electrode. A schematic of the working electrode assembly is presented in Figure S1 of the Supporting Information. All depositions took place at 0.6 V versus Ag/AgCl in an aqueous solution of 0.1 M manganese acetate. After the deposition was complete, the PET film was removed from the tape and was soaked in an aqueous etching solution (0.6 M KI and 0.075 M I_2) to remove any residual gold without damaging the manganese oxide within the pores. Removing gold was necessary for performing ion current measurements through the deposited MnO_2 mesorods.

dx.doi.org/10.1021/jp408107z | J. Phys. Chem. C 2013, 117, 24836–24842

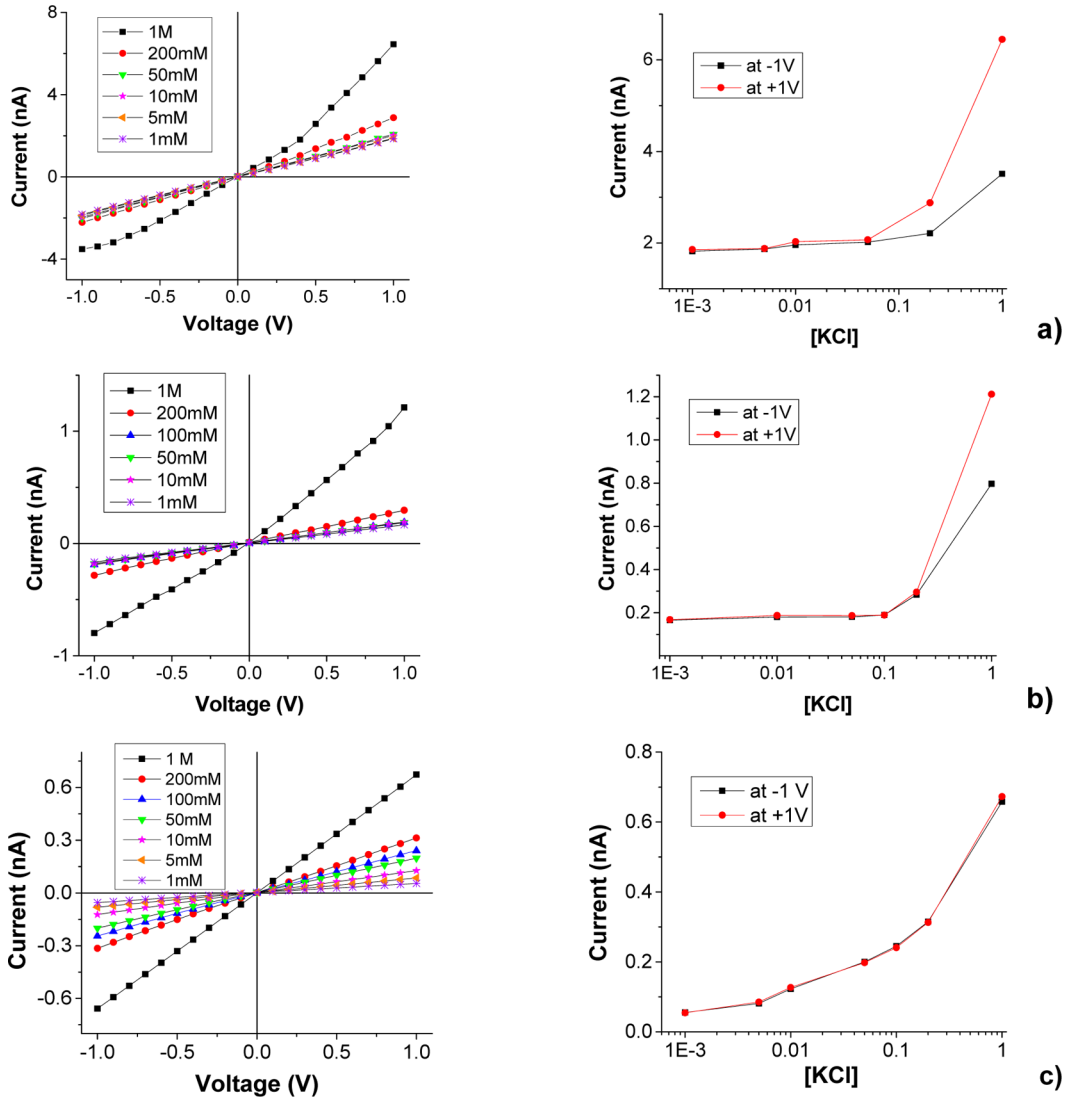

Figure 3. (a, b, left panels) Current−voltage curves in KCl recorded through single pores with deposited 200 nm long manganese oxide mesorods. The pore diameter before MnO_2 deposition was (a) 374 and (b) 304 nm. The presented data are averages over three independent voltage scans. (a, b, right panels) Absolute values of ion currents recorded at −1 V and +1 V. (c) Current−voltage curves through an empty cylindrical pore with an opening of 50 nm; this pore was not filled with manganese oxide. Absolute values of currents at ±1 V as a function of KCl concentration are shown in the right panel. All KCl solutions were buffered to pH 8.

Because of the challenges of microscopy characterization of single pores, the imaging was carried out on rods prepared according to the same procedure but using porous anodized aluminum oxide (AAO) membranes (Whatman, Maidstone, Kent, U.K.) in place of the PET films. The AAO pores are 200 nm in diameter, making them comparable to the single PET pores used for MnO_2 deposition and for ion current studies. With a pore density of ~10^9 cm^{-2}, AAO membranes allow preparation of many mesorods and their imaging, while maintaining similar confinement and morphology of the pores as in the polymer film. Moreover, AAO membranes can be dissolved in relatively mild chemical conditions (3 M NaOH) leaving intact, freestanding arrays of MnO_2 wires as seen in Figure 1. Because of variation in the diameter of the single pores in the PET films, the recorded current was not considered to be an accurate indicator of the total length of the mesorods as their density is unknown. Instead, the thickness of the deposited material was controlled by the deposition time. Using mesorods deposited in AAO membranes, the relationship between length and deposition time was characterized through scanning electron microscopy (SEM); a linear relationship was demonstrated between the growth time of the manganese oxide and the length of the resulting wires. As an example, deposition of 200 nm long MnO_2 rods was performed within half a minute. Slow deposition of MnO_2 is believed to allow for a complete filling of the pore cross-sectional area with the oxide.

3. RESULTS AND DISCUSSION

Figure 2 shows current−voltage curves recorded before and after deposition of ~200 nm long MnO_2 rods in two membranes containing single pores with an opening diameter of 374 and 304 nm, respectively, as measured from current−voltage curves. Deposition of MnO_2 significantly increased resistance of the two membranes. In case of the pore shown in Figure 2a, the resistance increased 7 times. Thus, assuming a cylindrical shape of the pore, the effective pore opening diameter decreased ~2.5 times. In the case of the structure in

dx.doi.org/10.1021/jp408107z | J. Phys. Chem. C 2013, 117, 24836−24842

Figure 2b, the increase in resistance was ~60 fold, indicating that the effective diameter after MnO_2 deposition was reduced to ~40 nm. The increase of the system resistance can be explained either by a restriction of the pore size because of the growth of solid metal oxide in the pore or by the formation of a meshlike porous structure with multiple pore openings significantly smaller than 140 or 40 nm. Imaging suggests that the deposited manganese oxide does not form tubular structures (see inset of Figure 1a) but rather creates porous rods. Ionic current measurements (see below) further corroborated a meshlike character of the deposited MnO_2. This random porous structure may also account for the variation in the magnitude of the resistance increase after MnO_2 deposition, despite the very similar ionic properties of the various samples, discussed further below. We tested nine independently prepared devices, and the increase of the system resistance after MnO_2 deposition varied between a factor of 4 and 125.

To confirm that the voids are smaller than the nominal 140 and 40 nm openings suggested and to estimate the size of the voids within the porous network, we performed a series of current−voltage measurements in aqueous solutions of KCl, NaCl, and LiCl in the range of concentrations from 1 mM to 1 M. If the surface of MnO_2 is charged, as suggested by the earlier studies,[21] and if the voids are of nanometer scale, one should observe ion current saturation at low concentrations of electrolyte. The electroneutrality requirement predicts that the difference in counterion and co-ion concentration will depend on the surface charge, σ, and the pore opening radius, r:[22]

$$C_+ - C_- = \Delta C = -2\sigma/er \quad (1)$$

where e is the elementary charge. The concentrations C_+ and C_- are, however, a strong function of the thickness of the electrical layer and, thus, of the concentration of the bulk electrolyte.[22] Below the concentration at which the pore radius approaches the thickness of the electrical double layer, only counterions are present in the pore, and the measured current becomes bulk concentration independent.

Figure 3a shows current−voltage curves through a MnO_2 rod deposited in a 374 nm in diameter single pore recorded in KCl. Recordings in NaCl and LiCl are shown in the Supporting Information (Figure S2) and exhibit the same characteristics. All solutions were buffered to pH 8. Ion currents started to saturate for both voltage polarities in ~50 mM, where the electrical double-layer thickness calculated as 0.3 nm/$\sqrt{c}$, with c expressed as mol/liter, is ~1.3 nm.[23] The expression was obtained for room temperature and dielectric constant of water equal to the bulk value of 80. It is known, however, that the confined space of nanopores can lower the dielectric constant of water,[24] implicating a thinner electrical double layer and even smaller effective opening diameter of the voids. The measurements, therefore, suggest that the effective diameter of the voids is just a few nanometers.

Figure 3b shows current−voltage curves through a 200 nm long MnO_2 wire deposited in a 304 nm pore. The currents started to saturate at a similar value of KCl concentration as in the case of the device created on the basis of a 374 nm pore, ~0.1 M (Figure 3a, b). This result confirms that the voids in the MnO_2 rods are roughly the same size, independent of the diameter of the pore in which they were deposited. An example of another MnO_2 mesorod with length of 1100 nm is shown in the Supporting Information. The absolute values of currents through different rods can vary significantly (Figure 3a, b and Figure S3 of the Supporting Information), which most probably results from a different number of voids in independently prepared mesorods. The variability of the number of voids is expected because of a relatively small diameter of the rods. Thus, the current through rods of different lengths does not always follow the behavior expected for a resistor. The nanometer scale and comparable size of the voids in different samples is, however, evidenced by a similar value of salt concentration at which the currents saturate for different, independently prepared, MnO_2 rods.

To provide evidence that the recorded current is indeed through the voids and not a pore of a size equal to the effective opening diameter calculated after MnO_2 deposition, we recorded $I-V$ curves through an empty cylindrical pore with an opening of 50 nm (Figure 3c). As expected, the ion current decreased monotonically with the decrease of the KCl concentration, and no saturation of ion currents was observed.

As the next step, we wanted to investigate the possibility that ions might pass through a constriction between a rod and pore walls. Such constriction could be present if the deposition did not fill the pore completely. Understanding the potential contribution of ionic transport through such gaps to the total measured current is important because the polymer walls are also negatively charged at pH 8; thus, if the gaps are present and are sufficiently narrow, saturation of the measured currents would be observed as well. We calculated an expected magnitude of the current through a 5 nm thick constriction placed between a 200 nm long rod deposited in a 304 nm diameter pore to be 40 nA in 1 M KCl, at 1 V, and, thus, 40 times higher than the measured values (see Figure 3b). We assumed that the constriction zone had a cross section of a disc with outer diameter of 304 nm and with inner diameter of 299 nm; the constriction zone was connected in series with the remaining 11.8 μm unfilled pore. Changing the inner diameter to 302 nm, thus reducing the size of the gap to 2 nm, gave a current of 27 nA, still much larger than the experimentally recorded currents. Performing the same calculations of ion current through a gap, which potentially could exist between a rod and pore walls in a pore with an opening diameter of 374 nm, also yielded much higher currents compared to experimentally found values. These calculations support our hypothesis that the measured currents are primarily due to ions passing through MnO_2.

Measurements of ion currents at pH 8 and pH 4 provided further evidence that the current probes the properties of the deposited mesorods and not of the polymer matrix. Figure 4 compares values of ion currents at 1 V recorded at pH 8 and pH 4 in 1 mM KCl and 1 mM LiCl through a MnO_2 rod deposited in a 240 nm diameter pore. Four orders of magnitude change in the proton concentration resulted in ~15% reduction of the current suggesting that (1) voids in MnO_2 are charged at pH 8 and pH 4, (2) ionic concentrations in the voids are determined by their surface charges, and (3) protons do not significantly contribute to the measured current. pH 4 is, however, close to the isoelectric point of PET surface; thus, currents through PET nanopores at these conditions are determined by the bulk concentration of the electrolyte and, in general, are significantly lower compared to the recordings at pH 8.[11,25−27] pH dependence of currents through PET pores is especially pronounced in low concentrations of the background electrolyte; in 1 mM KCl, lowering the pH to 3.5 reduced the ion current by a factor of ~2.[11] A weak pH dependence of the

dx.doi.org/10.1021/jp408107z | J. Phys. Chem. C 2013, 117, 24836−24842

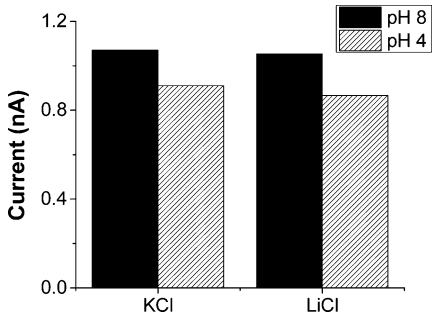

Figure 4. Values of currents at 1 V through a manganese oxide rod deposited in a 240 nm pore recorded in 1 mM KCl and 1 mM LiCl buffered to pH 8 and pH 4. The error bars are 10 pA and are not visible on this graph.

currents recorded for pores with deposited MnO_2 (Figure 4) gives us confidence that possible contribution of currents through gaps between polymer walls and a rod is insignificant. The measurements were not done beyond pH 4 because a few studies indicated a lack of structural stability of MnO_2 at pH 3.[28,29]

Measurements presented in Figure 4 also indicate that the currents through MnO_2 mesorods do not always follow bulk conductivities of the electrolytes since currents in LiCl are comparable to the currents in KCl. We do not yet have an explanation for this.

Current–voltage curves recorded in symmetric electrolyte conditions revealed saturation of ion currents suggesting that the MnO_2 voids carry finite surface charge. These measurements cannot, however, determine the polarity of the surface charges (positive or negative) or whether the surface charges make the voids selective for certain types of ions. To address these questions, we have used an approach often applied in electrophysiology for studying ionic selectivity of biological channels.[13,14] The measurement involves placing a porous structure in a conductivity cell whose two chambers are filled with KCl of different concentrations. If a pore is selective to cations or anions, the I–V curve will be shifted left or right along the voltage x-axis. This is a result of the electric potential difference which develops across the membrane to prevent diffusive movement of counterions (to the charges on the pore walls) from the side with a higher KCl concentration to the side with a lower KCl concentration. The potential difference at which the transmembrane current goes to zero is called a reversal potential (V_{rev}). The value and sign of the potential difference is related to the ratio of diffusion coefficients of potassium and chloride ions in the pore (D^{K}_{pore}, D^{Cl}_{pore}) by the Goldman–Hodgkin–Katz equation (eq 2)[14]

$$V_{rev} = \frac{RT}{F}\ln\frac{x[K^+]_1 + [Cl^-]_2}{x[K^+]_2 + [Cl^-]_1} \quad \text{where } x = \frac{D^{K}_{pore}}{D^{Cl}_{pore}} \tag{2}$$

where R is the gas constant, T is the temperature, and F is the Faraday constant. In our experimental configuration, the working electrode is on the side of the membrane with MnO_2; recording positive V_{rev} when the KCl concentration on side 1 is 0.1 M and on side 2 is 10 mM indicates cation selectivity. When the concentration gradient switches direction (i.e., 1 is a lower concentration than 2), a sign change should be observed in the reversal potential. The same reasoning and signs of reversal potential apply when LiCl is used as an electrolyte, and $x = D^{Li}_{pore}/D^{Cl}_{pore}$.

If the membrane is entirely rejecting one type of ion (e.g., anions), the magnitude of the measured potential difference is equal to Nernst potential, 58 mV for 10-fold concentration gradient at room temperature. If the membrane is not selective, the potential difference will be zero. Values of reversal potential between the two extreme values suggest partial cation (anion) selectivity of the structure expressed by the ratio x of diffusion coefficients of the two ions in the pore.

Ionic selectivity of a MnO_2 rod was first investigated in the concentration gradient set by 10 mM and 0.1 M KCl (Figure 5). The direction of the concentration gradient and the KCl concentration in contact with the mesorod could be controlled since the side of the membrane from which the MnO_2

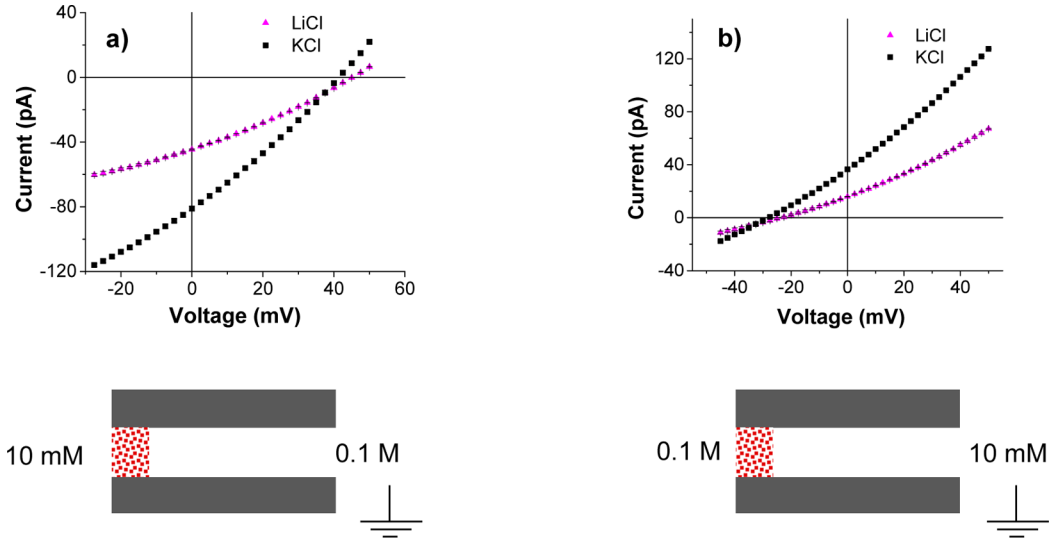

Figure 5. Current–voltage curves recorded when a single pore with deposited manganese oxide was placed in contact with a concentration gradient of KCl (black squares) or LiCl (magenta triangles). Panels a and b present data when the side of the membrane with deposited manganese oxide (marked as red mesh in the scheme) is in contact with a (a) lower or (b) higher concentration of an electrolyte, respectively. This pore before deposition of manganese oxide had an opening diameter of 270 nm. The presented data are averages of three voltage scans.

dx.doi.org/10.1021/jp408107z | J. Phys. Chem. C 2013, 117, 24836–24842

deposition was performed was marked. A nonzero reversal potential was observed, and its polarity indicated that MnO_2 was indeed cation selective. As an example, in Figure 5a recorded when the side with deposited MnO_2 was in contact with 10 mM KCl, an electric potential difference was created which pulled the cations toward the solution with a higher concentration of 0.1 M KCl. In our electrode configuration, it is the positive voltage that has to be applied to counterbalance the built-up potential difference. When the concentration gradient was switched, that is, the side with MnO_2 was in contact with 0.1 M KCl, the sign of the reversal potential switched as well. The transmembrane current was zero for +40 mV and −30 mV when the lower or higher salt concentration was placed at the MnO_2 deposited side, respectively (Figure 5 a, b). The ratios of diffusion coefficients of potassium and chloride ions in the pore $x = D^{Li}_{pore}/D^{Cl}_{pore}$ determined for these two V_{rev} values are 10 and 5, both indicating a cation selectivity and negative surface charges of the voids. The difference in the two values can be accounted for by the difference in the electrolyte configuration; the MnO_2 rod is in direct contact with the lower concentration solution in the first experiment but is in contact with the higher concentration solution in the second (Figure 5).

This difference in the magnitude of the reversal potential when changing the direction of the salt concentration gradient provides additional evidence for the presence of a meshlike structure of the deposited MnO_2. When the MnO_2 structure is in contact with a lower KCl concentration, the voids' transport properties are almost entirely dominated by the electrical double layer; thus, the structure is highly cation selective. In the opposite case, MnO_2 is in contact with 0.1 M KCl, and the double layer is thinner, leading to a smaller difference in the concentration between cations and anions in the voids compared to the previous situation, when MnO_2 was in contact with 10 mM KCl. An existence of different magnitudes of reversal potential for two different concentration gradient directions was previously observed for a conically shaped nanopore[30] and for an asymmetric biological pore OmpF.[13]

Recordings of reversal potential in LiCl revealed similar ion selectivity properties of MnO_2 as those observed with KCl (Figure 5). Because Ag/AgCl electrodes used in these measurements contained salt bridges filled with 3 M KCl, the junction potential, as calculated from the Henderson equation, is only 1.7 mV.[20] Almost identical cation selectivity of the mesorods in KCl and LiCl is in agreement with the observation of ion current saturation observed with all studied monovalent metal cations (Figure 3, Figure S2 of the Supporting Information).

Measurements of current−voltage curves at pH 8 and pH 4 (see Figure 4) suggest that the voids in MnO_2 carry negative charges even at the acidic conditions. To confirm this result, we performed reversal potential measurements at this pH in both KCl and LiCl. Finite values of reversal potential of ∼20 mV indicate that the MnO_2 voids are indeed negatively charged and further corroborate our hypothesis that the recorded currents are due to ions passing through the porous mesorods. The negative surface charge of MnO_2 at pH 4 is also in agreement with earlier experiments showing that the material loses its charge only at pH 2.[21]

Cation selectivity and the nanometer scale of the voids in the deposited MnO_2 structures also explain why in some recordings the current−voltage curves were nonlinear. A pore with MnO_2 creates an asymmetric structure with different openings on both sides of the membrane. Asymmetric nanopores with excess surface charges were reported to rectify the current with the preferential direction of the counterions' flow from the narrow opening toward the wider opening of the pore.[27,31−34] In our electrode configuration, the rectification shown in Figure 3 and Figure S2 of the Supporting Information is consistent with the earlier observations.

4. CONCLUSIONS

In this manuscript, we describe a method to probe structural and physical properties of porous manganese oxide by ionic current. The current carried by ions through the porous structure gives information on the effective size of the voids, the presence and polarity of surface charges, and the relative currents carried by different monovalent ions. We studied amorphous manganese oxide electrodeposited in single pores in a polymer film. The presented experiments revealed the effective size of the voids to be less than 5 nm and revealed the presence of negative surface charge inside the mesh void structure.

Our future experiments will focus on understanding ionic transport through manganese oxide at different oxidation states of the material. Ion current through MnO_2 will allow us to answer questions about whether the effective size of the voids and their surface charge change during charging/discharging of the material.

■ ASSOCIATED CONTENT

Ⓢ Supporting Information

Scheme of the experimental setup used for deposition of mesorods, current−voltage curves through a 200 nm long MnO_2 rod in solutions of NaCl and LiCl, and recordings through an 1100 nm long rod in KCl. This material is available free of charge via the Internet at http://pubs.acs.org.

■ AUTHOR INFORMATION

Corresponding Authors

*E-mail: slee@umd.edu. Phone: 301-405-7906.
*E-mail: zsiwy@uci.edu. Phone: 949-824-8290.

Author Contributions

The manuscript was written through contributions of all authors. All authors have given approval to the final version of the manuscript.

Notes

The authors declare no competing financial interest.

■ ACKNOWLEDGMENTS

Irradiation with swift heavy ions was performed at the GSI Helmholtzzentrum für Schwerionenforschung GmbH, Darmstadt, Germany. This research was supported by the Nanostructures for Electrical Energy Storage, an Energy Frontier Research Center funded by the U.S. Department of Energy, Office of Science, Office of Basic Energy Sciences (award no. DESC0001160).

■ REFERENCES

(1) Patzke, G.; Zhou, Y.; Kontic, R.; Conrad, F. Oxide Nanomaterials: Synthetic Developments, Mechanistic Studies, and Technological Innovations. *Angew. Chem., Int. Ed.* **2011**, *50*, 826−859.

(2) Marom, R.; Amalraj, S. F.; Leifer, N.; Jacob, D.; Aurbach, D. A Review of Advanced and Practical Lithium Battery Materials. *J. Mater. Chem.* **2011**, *21*, 9938−9954.

(3) Simon, P.; Gogotsi, Y. Materials for Electrochemical Capacitors. *Nat. Mater.* **2008**, *7*, 845−854.

(4) Arico, A. S.; Bruce, P.; Scrosati, B.; Tarascon, J. M.; Van Schalkwijk, W. Nanostructured Materials for Advanced Energy Conversion and Storage Devices. *Nat. Mater.* **2005**, *4*, 366−377.
(5) Liu, C.; Li, F.; Ma, L.-P.; Cheng, H.-M. Advanced Materials for Energy Storage. *Adv. Mater.* **2010**, *22*, E28−E62.
(6) Kang, S. H.; Goodenough, J. B.; Rabenberg, L. K. Nanocrystalline Lithium Manganese Oxide Spinel Cathode for Rechargeable Lithium Batteries. *Electrochem. Solid-State Lett.* **2001**, *4*, A49−A51.
(7) Tang, W.; Wang, X. J.; Hou, Y. Y.; Li, L. L.; Sun, H.; Zhu, Y. S.; Bai, Y.; Wu, Y. P.; Zhu, K.; Van Ree, T. Nano $LiMn_2O_4$ as Cathode Material of High Rate Capability for Lithium Ion Batteries. *J. Power Sources* **2012**, *198*, 308−311.
(8) Strobel, P.; Darie, C.; Thiéry, F.; Bacia, M.; Proux, O.; Ibarra-Palos, A.; Soupart, J. B. New Nanocrystalline Manganese Oxides as Cathode Materials for Lithium Batteries: Electron Microscopy, Electrochemical and X-ray Absorption Studies. *Solid State Ionics* **2006**, *177*, 523−533.
(9) Sherrill, S. A.; Duay, J.; Gui, Z.; Banerjee, P.; Rubloff, G. W.; Lee, S. B. MnO_2/TiN Heterogeneous Nanostructure Design for Electrochemical Energy Storage. *Phys. Chem. Chem. Phys.* **2011**, *13*, 15221−15226.
(10) Wei, W.; Cui, X.; Chen, W.; Ivey, D. Manganese Oxide-Based Materials as Electrochemical Supercapacitor Electrodes. *Chem. Soc. Rev.* **2011**, *40*, 1697−1721.
(11) Wolf, A.; Reber, N.; Apel, P. Yu.; Fischer, B. E.; Spohr, R. Electrolyte Transport in Charged Single Ion Track Capillaries. *Nucl. Instrum. Methods Phys. Res., Sect. B* **1995**, *105*, 291−293.
(12) Stein, D.; Kruithof, M.; Dekker, C. Surface-Charge-Governed Ion Transport in Nanofluidic Channels. *Phys. Rev. Lett.* **2004**, *93*, 035901−035905.
(13) Alcaraz, A.; Nestorovich, E. M.; Aguilella-Arzo, M.; Aguilella, V. M.; Bezrukov, S. M. Salting Out the Ionic Selectivity of a Wide Channel: The Asymmetry of OmpF. *Biophys. J.* **2004**, *87*, 943−957.
(14) Hille, B. *Ion Channels of Excitable Membranes*, 3rd ed.; Sinauer Associates: Sunderland, MA, 2001.
(15) Fleischer, R. L.; Price, P. B.; Walker, R. M. *Nuclear Tracks in Solids: Principles and Applications*; University of California Press: Berkeley, CA, 1975.
(16) Spohr, R. Methods and Device to Generate a Predetermined Number of Ion Tracks. German Patent DE 2951376 C2, 1983; U.S. Patent 4,369,370, 1983.
(17) Powell, M. R.; Vlassiouk, I.; Martens, C.; Siwy, Z. S. Nonequilibrium 1/*f* Noise in Rectifying Nanopores. *Phys. Rev. Lett.* **2009**, *103*, 248104−248107.
(18) Bezrukov, S. M.; Vodyanoy, I. Probing Alamethicin Channels With Water-Soluble Polymers. Effect on Conductance of Channel States. *Biophys. J.* **1993**, *64*, 16−25.
(19) Verdia-Baguena, C.; Queralt-Martin, M.; Aguilella, V. M.; Alcaraz, A. Protein Ion Channels as Molecular Ratchets. Switchable Current Modulation in Outer Membrane Protein F Porin Induced by Millimolar La^{3+} Ions. *J. Phys. Chem. C* **2012**, *116*, 6537−6542.
(20) Perram, J. W.; Stiles, P. J. On the Nature of Liquid Junction and Membrane Potentials. *Phys. Chem. Chem. Phys.* **2006**, *8*, 4200−4213.
(21) Murray, J. W. The Surface Chemistry of Hydrous Manganese Dioxide. *J. Colloid Interface Sci.* **1974**, *46*, 357−371.
(22) Vlassiouk, I.; Smirnov, S.; Siwy, Z. S. Ion Selectivity of Single Nanochannels. *Nano Lett.* **2008**, *8*, 1978−1985.
(23) Israelachvili, J. N. *Intermolecular and Surface Forces*, 2nd ed.; Academic Press: London, 1991.
(24) Senapati, S.; Chandra, A. Dielectric Constant of Water Confined in a Nanocavity. *J. Phys. Chem. B* **2001**, *105*, 5106−5109.
(25) Ermakova, L. E.; Sidorova, M. P.; Bezrukova, M. E. Filtration and Electrokinetic Characteristics of Track Membranes. *Colloid J. Russ. Acad.* **1998**, *60*, 705−712.
(26) Yameen, B.; Ali, M.; Neumann, R.; Ensinger, W.; Knoll, W.; Azzaroni, O. Proton-Regulated Rectified Ionic Transport Through Solid-State Conical Nanopores Modified with Phosphate-Bearing Polymer Brushes. *Chem. Commun.* **2010**, *46*, 1908−1910.
(27) Siwy, Z. Ion Current Rectification in Nanopores and Nanotubes with Broken Symmetry Revisited. *Adv. Funct. Mater.* **2006**, *16*, 735−746.
(28) Xu, C.; Wei, C.; Li, B.; Kang, F.; Guan, Z. Charge Storage Mechanism of Manganese Dioxide for Capacitor Application: Effect of the Mild Electrolytes Containing Alkaline and Alkaline-Earth Metal Cations. *J. Power Sources* **2011**, *196*, 7854−7859.
(29) Bakardjieva, S.; Bezdicka, P.; Grygar, T.; Vorm, P. Reductive Dissolution of Microparticulate Manganese Oxides. *J. Solid State Electrochem.* **2000**, *4*, 306−313.
(30) Siwy, Z.; Kosinska, I. D.; Fulinski, A.; Martin, C. R. Asymmetric Diffusion Through Synthetic Nanopores. *Phys. Rev. Lett.* **2005**, *94*, 048102−048105.
(31) Wei, C.; Bard, A. J.; Feldberg, S. W. Current Rectification at Quartz Nanopipet Electrodes. *Anal. Chem.* **1997**, *69*, 4627−4633.
(32) Apel, P. Yu; Korchev, Y. E.; Siwy, Z.; Spohr, R.; Yoshida, M. Diode-Like Single-Ion Track Membrane Prepared by Electro-Stopping. *Nucl. Instrum. Methods Phys. Res., Sect. B* **2001**, *184*, 337−346.
(33) Siwy, Z.; Fulinski, A. Fabrication of a Synthetic Nanopore Ion Pump. *Phys. Rev. Lett.* **2002**, *89*, 198103−198107.
(34) White, H. S.; Bund, A. Ion Current Rectification at Nanopores in Glass Membranes. *Langmuir* **2008**, *24*, 2212−2218.